THE JOURNAL OF BIOLOGICAL CHEMISTRY VOL. 281, NO. 18, pp. 12760–12766, May 5, 2006

A Trans-tail Histone Code Defined by Monomethylated H4 Lys-20 and H3 Lys-9 Demarcates Distinct Regions of Silent Chromatin*[S]

Received for publication, December 19, 2005, and in revised form, February 10, 2006 Published, JBC Papers in Press, March 3, 2006, DOI 10.1074/jbc.M513462200

Jennifer K. Sims, Sabrina I. Houston, Tanya Magazinnik, and Judd C. Rice[1]

From the Department of Biochemistry and Molecular Biology, USC/Norris Comprehensive Cancer Center, University of Southern California Keck School of Medicine, Los Angeles, California 90033

The specific post-translational modifications of the histone proteins are associated with specific DNA-templated processes, such as transcriptional activation or repression. To investigate the biological role(s) of histone H4 lysine 20 (H4 Lys-20) methylation, we created a novel panel of antibodies that specifically detected mono-, di-, or trimethylated H4 Lys-20. We report that the different methylated forms of H4 Lys-20 are compartmentalized within visually distinct, transcriptionally silent regions in the mammalian nucleus. Interestingly, direct comparison of methylated H4 Lys-20 with the different methylated states of histone H3 lysine 9 (H3 Lys-9) revealed significant overlap and exclusion between the specific groups of methyl modifications. Trimethylated H4 Lys-20 and H3 Lys-9 were both selectively enriched within pericentric heterochromatin. Similarly, monomethylated H4 Lys-20 and H3 Lys-9 partitioned together and the dimethylated forms partitioned together within the chromosome arms; however, the mono- and dimethylated modifications were virtually exclusive. These findings strongly suggest that the combinatorial presence or absence of the different methylated states of H4 Lys-20 and H3 Lys-9 define particular types of silent chromatin. Consistent with this, detailed analysis of monomethylated H4 Lys-20 and H3 Lys-9 revealed that both were preferentially and selectively enriched within the same nucleosome particle *in vivo*. Collectively, these findings define a novel trans-tail histone code involving monomethylated H4 Lys-20 and H3 Lys-9 that act cooperatively to mark distinct regions of silent chromatin within the mammalian epigenome.

Within eukaryotic nuclei, DNA associates with nuclear proteins to form chromatin. The most fundamental structural unit of chromatin, the nucleosome, is composed of ~146 bp of DNA wrapped around an octamer of the core histone proteins H2A, H2B, H3, and H4 (1). Although much has been elucidated about chromatin in the last decade, it remains unclear how distinct functional domains of chromatin are established and maintained within living cells. It is well known that chromatin function is modulated, at least in part, by enzymes that post-translationally modify specific amino acids on the histone proteins (2). Such post-translational modifications include acetylation, phosphorylation, ubiquitination, and methylation (3). Increasing evidence indicates that specific covalent modifications, alone or in combination, directly participate in specific downstream nuclear processes including transcription, replication, and repair (4). Thus, it is theorized that this "histone code" may serve to establish and maintain distinct functional domains that are epigenetically transmitted (5–7).

One histone modification that has received increased attention is the methylation of lysine 20 on histone H4 (H4 Lys-20).[2] Although this methylated histone lysine residue was identified over 40 years ago, the biological significance of this modification has remained enigmatic (8). Investigations into H4 Lys-20 methylation were complicated by the fact that the epsilon amino group of lysine residues can be mono-, di-, or trimethylated *in vivo* (9). The recent discovery of the histone methyltransferase enzymes (HMTs) responsible for making the specific H4 Lys-20 methyl modifications have led to important insights into their potential biological functions (10–12). PR-Set7, also known as Set8, is responsible for the majority of monomethylated H4 Lys-20, whereas the Suv4-20 HMTs are responsible for the bulk of trimethylated H4 Lys-20 in flies and humans (12–15). Recent studies strongly suggest that H4 Lys-20 methylation and the HMTs that create these marks are involved in many important DNA-associated processes including transcriptional silencing, higher order chromatin structure, differentiation, genomic stability, and cell division (12, 16–21). In addition, a recent finding indicates that H4 Lys-20 methylation and the H4 Lys-20 HMT homologue in fission yeast play a role in DNA double-strand break repair, although this has yet to be confirmed in higher eukaryotes (22).

To further study the function(s) of the different methylated states of H4 Lys-20, we created a novel panel of H4 Lys-20 methyl-specific antibodies. Use of these antibodies in indirect immunofluorescence studies revealed that the mono-, di-, and trimethylated forms of H4 Lys-20 partitioned to distinct compartments of silent chromatin in the mammalian nucleus. Because we had previously observed similar partitioning of the methylated forms of histone H3 lysine 9 (H3 Lys-9) (23, 24), a direct comparison was made between the different methylated states of H4 Lys-20 and H3 Lys-9. Surprisingly, we discovered that there was a selective enrichment within the same silent nuclear compartments specifically for similar methylated states of H4 Lys-20 and H3 Lys-9. Consistent results were obtained on extended chromatin fibers. Further analysis revealed that monomethylated H4 Lys-20 and H3 Lys-9 were preferentially and selectively enriched on the same nucleosome core particles *in vivo*. Collectively, our findings indicate that a trans-tail his-

* This work was supported in part by Grant IRG-58-007-45 from the American Cancer Society and by the Robert E. and May R. Wright Foundation. The costs of publication of this article were defrayed in part by the payment of page charges. This article must therefore be hereby marked "*advertisement*" in accordance with 18 U.S.C. Section 1734 solely to indicate this fact.

[S] The on-line version of this article (available at http://www.jbc.org) contains a supplemental figure.

[1] A General Motors Cancer Research Scholar. To whom correspondence should be addressed: Dept. of Biochemistry and Molecular Biology, University of Southern California Keck School of Medicine, 1501 San Pablo St., ZNI 225, MC 2821, Los Angeles, CA 90033. Tel.: 323-442-4332; Fax: 323-442-4433; E-mail: juddrice@usc.edu.

[2] The abbreviations used are: H4 Lys-20, histone H4 lysine 20; H3 Lys-9, histone H3 lysine 9; H4 Lys-16, histone H4 lysine 16; H2B Lys-123, histone H2B lysine 123; HMT, histone methyltransferase; MEF, mouse embryonic fibroblast; FITC, fluorescein isothiocyanate; DAPI, 4′,6-diamidino-2-phenylindole; pol, polymerase.

tone code involving monomethylated H4 Lys-20 and H3 Lys-9 exists in higher eukaryotes and is likely to play an important role in the formation of a specific repressive chromatin state.

EXPERIMENTAL PROCEDURES

Antibody Characterization and Western Analysis—For antibody characterization, 200 ng of recombinant human histone H4, 2 μg of acid-extracted chicken histones, and whole cell lysates from 10^5 HeLa cells were fractionated by SDS-PAGE, transferred to polyvinylidene difluoride, blocked in 5% nonfat milk/Tris-buffered saline, and incubated with the H4 Lys-20 mono- (1:150,000), di- (1:100,000), or trimethyl (1:20,000) antibodies in 1% nonfat milk/Tris-buffered saline for 1 h rotating at room temperature. Following three washes in Tris-buffered saline + 0.1% Tween 20, blots were incubated with a horseradish peroxidase-conjugated anti-rabbit antibody (1:5,000) in 1% nonfat milk/Tris-buffered saline for 1 h at room temperature prior to the addition of ECL Plus (Amersham Biosciences). Results were visualized by exposure to film for 1 min. For competition experiments, each antibody was preincubated with 1 μg of each peptide for 1 h rotating at room temperature before addition to the polyvinylidene difluoride membrane containing whole cell lysate from 10^5 HeLa cells. The linear peptides used for these studies correspond to residues 16–25 of histone H4.

Immunofluorescence—Mouse embryonic fibroblasts (MEFs) were prepared, fixed, and stained as described previously (24). Antibody dilutions used were as follows: H4 Lys-20 mono- (1:1,000), di- (1:500), and trimethyl (1:1,000); H3 Lys-9 mono- (1:1,000; Upstate), di- (1:2,000; Upstate), and trimethyl (1:1,000; Upstate); RNA pol II (1:1,000, Covance). Dual staining was performed as described previously (24). Staining was visualized using a ×63 objective on a Zeiss LSM 510 dual-photon confocal microscope. Pictures were analyzed using Adobe PhotoShop CS2.

Chromatin Fibers—Chromatin fibers were prepared as described previously with the following modifications (25). Nuclei were extracted from HeLa cells using ice cold nuclear isolation buffer (150 mM NaCl, 10 mM HEPES, pH 7.4, 1.5 mM $MgCl_2$, 10 mM KCl, 0.5% Nonidet P-40, 0.5 mM dithiothreitol, protease inhibitors) and isolated by centrifugation. Nuclei were lysed in 25 mM Tris, pH 7.5, 0.5 M NaCl, 1% Triton X-100, and 0.5 M urea to liberate chromatin that was spread onto supercharged microscope slides (VWR) and fixed in 4% paraformaldehyde/phosphate-buffered saline for 20 min at room temperature. Slides were blocked in phosphate-buffered saline containing 1% bovine serum albumin and 0.5% Triton X-100 for 1 h at 37 °C. Primary antibodies were diluted 1:100 in blocking solution and applied to slides followed by an overnight incubation at 4 °C. Slides were washed three times in 0.05% Triton X-100/phosphate-buffered saline prior to a 2-h room temperature incubation with secondary antibodies. Staining was visualized using a ×60 objective on a DeltaVision Spectris microscope, and images were taken with softWoRx (Applied Precision). Pictures were analyzed using Adobe PhotoShop CS2.

Immunoprecipitations—Nuclei obtained from HeLa cells were resuspended in micrococcal nuclease digestion buffer (0.32 M sucrose, 50 mM Tris-HCl, pH 7.4, 4 mM $MgCl_2$, 1 mM $CaCl_2$, 1 mM phenylmethylsulfonyl fluoride) to a concentration of 0.5 mg/ml as determined by A_{260}. Micrococcal nuclease was added to the nuclei (50 units/0.5 mg) and digested for 20 min at 37 °C. The reaction was stopped with 10 mM EDTA, and mononucleosomes were isolated by centrifugation. One hundred micrograms of mononucleosomes were incubated with 100 μl of the H4 Lys-20 monomethyl-specific antibody or 180 μl of the H4 Lys-20 trimethyl-specific antibody in micrococcal nuclease digestion buffer and precipitated with Pro-A-Sepharose beads (Amersham Biosciences). Beads were sequentially washed in phosphate-buffered saline containing 50, 100, or 150 mM NaCl. The bound material was eluted in Tris-EDTA, 1% SDS by intermittent vortexing for 30 min. SDS-PAGE was used to fractionate 2% of the input material and 5% of the eluted bound material, which was transferred to polyvinylidene difluoride and immunoblotted with the various methyl-specific antibodies.

RESULTS

Generation of Histone H4 Lys-20 Methyl-specific Antibodies—To determine the biological significance of the different states of H4 Lys-20 methylation, polyclonal antibodies were developed using twice-branched synthetic peptides engineered from amino acids 16–25 of the human histone H4 sequence containing a mono-, di-, or trimethylated Lys-20 residue (Fig. 1*A*) (26). Western analysis demonstrated that each antibody specifically detected only modified histone H4 as the antibodies failed to detect the unmodified recombinant histone H4 or any other cellular protein from HeLa whole cell lysates (Fig. 1*B*). To determine the H4 Lys-20 methyl specificity of each antibody, the modified peptides were used in peptide competition experiments as described previously (24). The results indicate that only the H4 Lys-20 mono-, di-, and trimethylated linear peptides were able to effectively absorb the appropriate signal of the H4 Lys-20 mono-, di-, and trimethyl antibodies, respectively (Fig. 1*C*). Similar experiments confirmed that the antibodies are also highly specific in immunofluorescence (see supplemental Fig. S1) and immunoprecipitation experiments (see Fig. 5).

One potential problem associated with modification-specific antibodies is "epitope masking," a phenomenon in which neighboring post-translational modifications hinder the ability of the antibody to effectively bind its epitope. To determine whether H4 Lys-16 acetylation, the nearest known potential modification to H4 Lys-20, could impair the ability of the antibodies to detect H4 Lys-20 methylation, histones were hyperacetylated using the yeast NuA4 complex (27, 28). Although significant increases in H4 Lys-16 acetylation were readily detected by Western analysis, the detection efficiency of our H4 Lys-20 methyl antibodies were unaffected by global increases in H4 Lys-16 acetylation (Fig. 1*D*). Therefore, antibodies specific to the mono-, di-, or trimethylated form of H4 Lys-20 were successfully generated and could be used confidently to investigate the biological relevance of each of these histone modifications.

Different Methylated States of H4 Lys-20 Partition to Distinct Silent Nuclear Compartments—To determine the nuclear localizations of each of the H4 Lys-20 methyl modifications, immunofluorescence experiments were performed in female MEFs using the methyl-specific antibodies. As shown in Fig. 2*A*, mono- and dimethylated H4 Lys-20 were distributed throughout the interphase nucleus but tended to be predominantly targeted to specific chromosomal regions, as evidenced by their intense punctate staining. Monomethylated H4 Lys-20 appeared to be enriched toward the nuclear periphery, was generally excluded from nucleoli, and was enriched within the facultative heterochromatin of the female inactive X chromosome (Figs. 2*B* and 3*A*) (29). In contrast, dimethylated H4 Lys-20 was dispersed fairly evenly throughout the nucleus, was consistently found in the nucleoli, and was not enriched on the inactive X chromosome. Both mono- and dimethyl modifications were excluded from the DAPI-dense constitutive heterochromatic pericentric foci, where trimethylated H4 Lys-20 was primarily localized (Fig. 2*A*) (30). To determine whether mono- and dimethylated H4 Lys-20 were found within similar nuclear compartments, dual staining experiments were performed as described previously (24). As shown in Fig. 2*B*, mono- and dimethylated H4 Lys-20 appear to be mutually exclusive as evidenced by the lack of co-staining.

Although it was clear that trimethylated H4 Lys-20 was enriched within constitutive heterochromatin, the speckling patterns observed

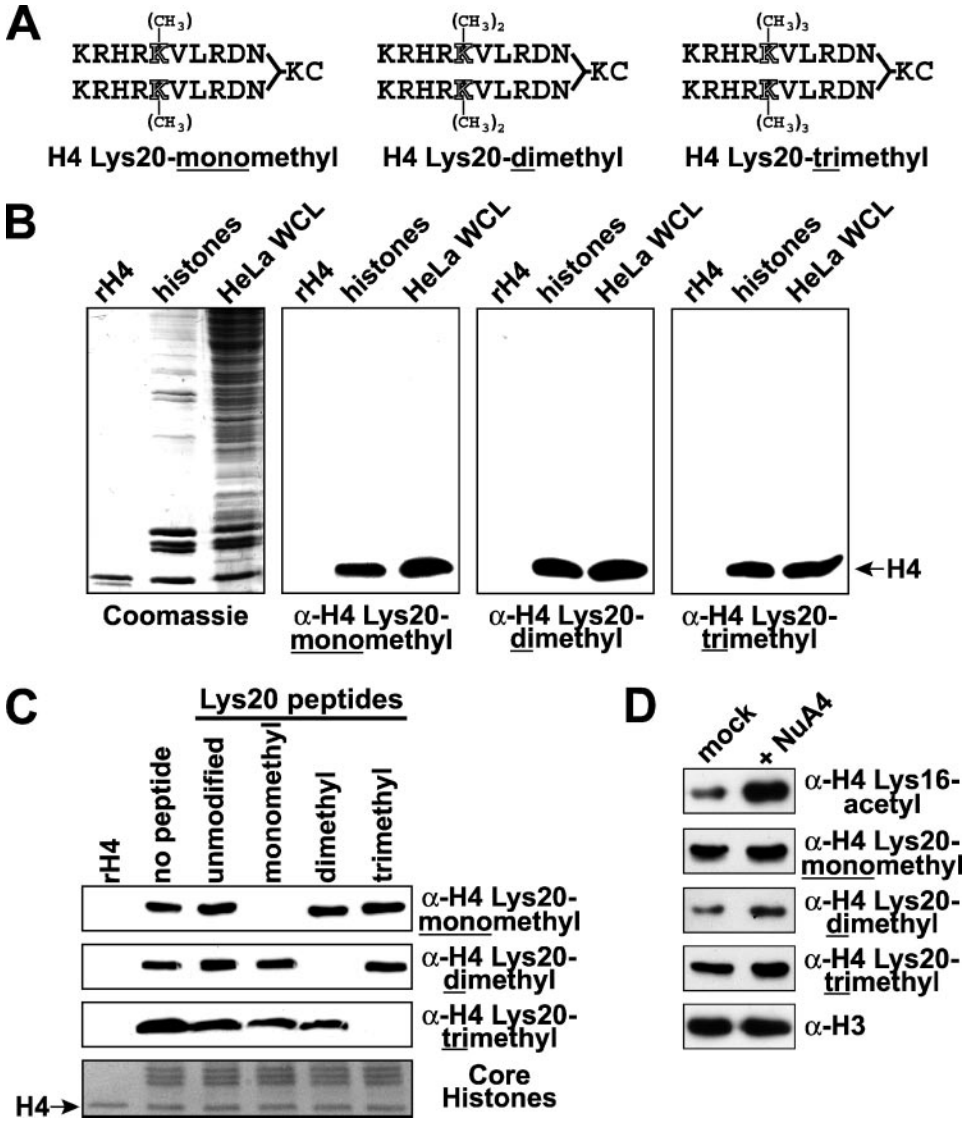

FIGURE 1. **Characterization of a novel panel of histone H4 Lys-20 methyl-specific antibodies.** *A*, schematic diagram of the twice-branched synthetic peptides used to generate the rabbit polyclonal H4 Lys-20 mono-, di-, and trimethyl-specific antibodies. *B*, Western analysis of the H4 Lys-20 methyl-specific antibodies using recombinant H4 (*rH4*), chicken histones, and HeLa whole cell lysates (*WCL*). Each antibody only detects modified H4 (*arrow*). *C*, peptide competition followed by Western analysis on HeLa whole cell lysates, using the different H4 Lys-20 methyl-specific antibodies with synthetic peptides that were unmodified or mono-, di-, or trimethylated at Lys-20. Each antibody is highly specific as only the appropriate corresponding peptide can eliminate the signal for each of the antibodies. *D*, HeLa core histones were hyperacetylated *in vitro* by incubation with the yeast NuA4 complex. Western analysis demonstrated that the global increase in H4 Lys-16 acetylation did not hinder the ability of the H4 Lys-20 methyl-specific antibodies to detect their epitope. *mock*, minus NuA4.

for mono- and dimethylated H4 Lys-20 were reminiscent of transcriptionally engaged chromatin. To determine whether these modifications were associated with active regions of the genome, dual staining experiments were performed with the methyl-specific antibodies and a monoclonal RNA pol II antibody (Fig. 2*A*). In all cases, RNA pol II was found evenly dispersed throughout the nucleus and was excluded from the nucleoli. Comparison with RNA pol II staining revealed that the majority of mono- and dimethylated H4 Lys-20 was excluded from transcriptionally active regions, as demonstrated by the lack of co-staining in the merged images, indicating that the majority of all forms of H4 Lys-20 methylation are enriched within silent chromatin. Collectively, these findings indicate that mono-, di-, and trimethylated H4 Lys-20 are each targeted to distinct transcriptionally inactive nuclear compartments.

Similar Methylated States of H4 Lys-20 and H3 Lys-9 Are Enriched within the Same Silent Nuclear Compartments—The differential nuclear localizations of the methylated forms of H4 Lys-20 were strikingly similar to the previously described localizations of the various methylated forms of H3 Lys-9 (23, 24). Based on this, we hypothesized that similar methylated states of H4 Lys-20 and H3 Lys-9 were targeted to the same silent nuclear compartments. To test this hypothesis, dual staining experiments were performed in MEFs using various combinations of the methyl-specific antibodies (Fig. 3). Consistent with previous reports, the bulk of both trimethylated H4 Lys-20 and trimethylated H3 Lys-9 was enriched within pericentric heterochromatin (Fig. 3*C*) (12, 30). Similar to trimethylation, the majority of monomethylated H4 Lys-20 was localized to the same nuclear compartments as monomethylated H3 Lys-9 (Fig. 3*A*). Although the overlap between monomethylated H4 Lys-20 and dimethylated H3 Lys-9 was detected, especially on the inactive X chromosome, co-localization was less pronounced when compared with monomethylated H3 Lys-9. Dimethylated H4 Lys-20 consistently appeared to preferentially co-localize to dimethylated H3 Lys-9 compartments when compared with monomethylated H3 Lys-9 (Fig. 3*B*). Although dimethylated H4 Lys-20 and H3 Lys-9 do partition to the same compartments, there also appeared to be many regions where these two modifications were mutually exclusive. In contrast, our results demonstrate that the majority of monomethylated H4 Lys-20 and H3 Lys-9 are enriched within the same transcriptionally silent nuclear compartments.

Similar Methylated States of H4 Lys-20 and H3 Lys-9 Are Enriched within the Same Regions along Chromatin Fibers—To examine the co-localization of these different repressive methyl modifications at higher resolution, dual staining experiments were performed on extended chromatin fibers from HeLa cells using the various methyl-specific anti-

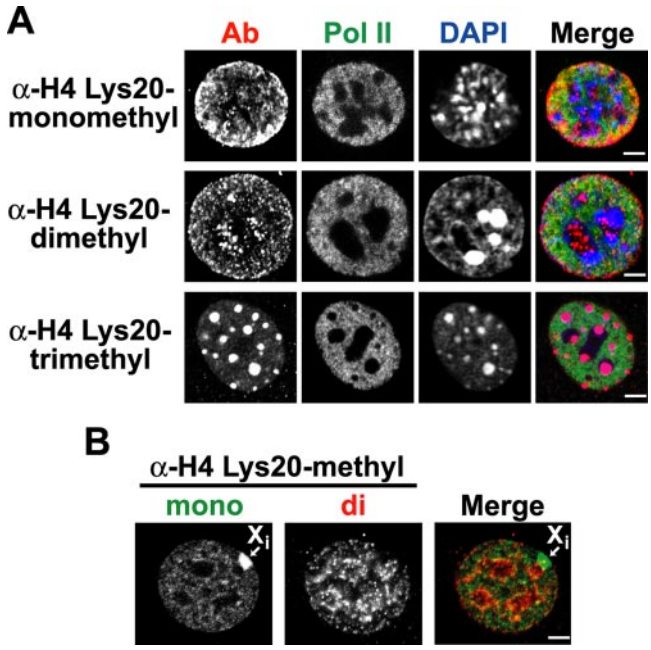

FIGURE 2. **The histone H4 Lys-20 methyl modifications are differentially enriched within distinct silent nuclear compartments.** *A*, immunofluorescence staining of MEFs using the H4 Lys-20 methyl-specific antibodies (*Ab*). H4 Lys-20 methylation is visualized as *red* (Cy3), RNA pol II is *green* (FITC), and DNA stained with DAPI is *blue*. The minor overlap between monomethylated H4 Lys-20 and RNA pol II is indicated by the *yellow regions* in the merged image. The co-localization of trimethylated H4 Lys-20 with the DAPI-dense pericentric heterochromatic regions is visualized as *purple* in the merged image. *B*, dual staining of monomethylated (*mono*, *red*) and dimethylated (*di*, *green*) H4 Lys-20 indicates that they are mutually exclusive, as demonstrated by the lack of overlap (*yellow*) in the merged image. The unique staining patterns of each methylated form of H4 Lys-20 indicate that they partition to distinct transcriptionally silent nuclear compartments within the mammalian nucleus. *Bar* = 5 μm.

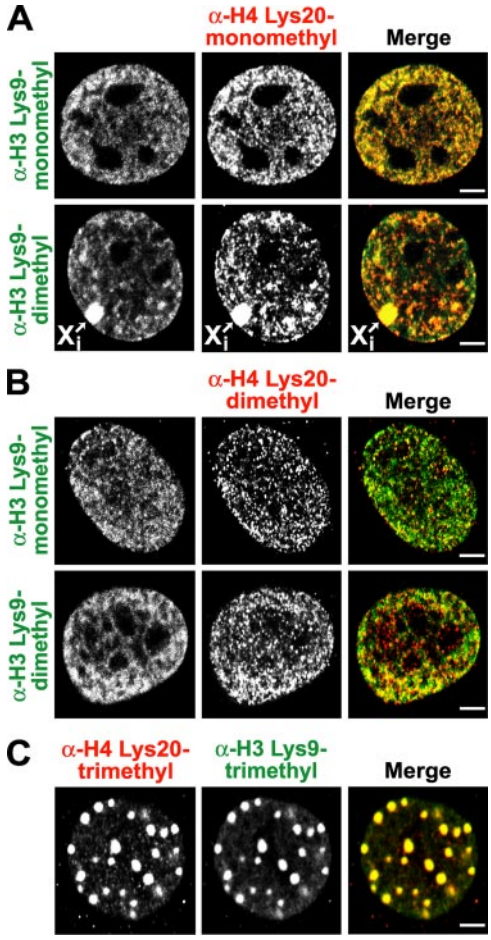

FIGURE 3. **Specific methylated states of H4 Lys-20 and H3 Lys-9 co-localize to the same silent nuclear compartments.** *A*, MEFs co-stained for monomethylated H4 Lys-20 (Cy3; *red*) and either mono- (*top panels*) or dimethylated (*bottom panels*) H3 Lys-9 (FITC, *green*). Monomethylated H4 Lys-20 and H3 Lys-9 are preferentially enriched within the same silent nuclear compartments as observed by the large amount of *yellow* in the merged image. In contrast, monomethylated H4 Lys-20 is mostly excluded from dimethylated H3 Lys-9 regions except on the inactive X chromosome (x_i). *B*, MEFs co-stained for dimethylated H4 Lys-20 (Cy3; *red*) and either mono- (*top panels*) or dimethylated (*bottom panels*) H3 Lys-9 (FITC; *green*). Dimethylated H4 Lys-20 and H3 Lys-9 co-localize to similar silent nuclear compartments (*yellow* in the merged image), although there are also regions where they are mutually exclusive. Dimethylated H4 Lys-20 does not co-localize to monomethylated H3 Lys-9 nuclear compartments. *C*, MEFs co-stained for trimethylated H4 Lys-20 (Cy3; *red*) and H3 Lys-9 (FITC; *green*). Both modifications are dramatically enriched within DAPI-dense pericentric heterochromatin. *Bar* = 5 μm.

bodies (Fig. 4). Similar to the findings in the MEF interphase nuclei, the monomethylated forms of H4 Lys-20 and H3 Lys-9 were preferentially targeted to the same silent regions along the chromatin fiber (Fig. 4*A*). The well defined punctate staining pattern of these monomethyl histone modifications strongly suggests that they are enriched within specific genomic regions, although these regions are currently undefined. It is important to note that although monomethylated H4 Lys-20 nearly always co-localized with monomethylated H3 Lys-9, monomethylated H3 Lys-9 was also found in silent regions along the chromatin fibers that were devoid of monomethylated H4 Lys-20 (Fig. 4*A*). In comparison, dimethylated H3 Lys-9 was more dispersed along the length of the chromatin fiber and, consistent with the findings in interphase nuclei, appeared to be preferentially enriched in the same dispersed regions as dimethylated H3 Lys-9 (Fig. 4*B*). Although dimethylated H4 Lys-20 also seemed to localize to some regions along the chromatin fibers that were enriched in monomethylated H3 Lys-9, closer examination of these regions revealed that dimethylated H4 Lys-20 was flanking the monomethylated H3 Lys-9 regions (Fig. 4*D*). Similar experiments were performed for trimethylated H4 Lys-20. Although we speculated that this modification was restricted to pericentric repeats, and thus, would be difficult to detect on chromatin fibers, trimethylated H4 Lys-20 was enriched within specific regions throughout the length of the fibers (Fig. 4*C*). As expected, trimethylated H3 Lys-9 co-localized to these regions. Unexpectedly, mono- and dimethylated H3 Lys-9 also co-localized to these regions, although much less frequently. Collectively, these results support the above findings and suggest that similar methylated states of H4 Lys-20 and H3 Lys-9 (*i.e.* mono-, di-, or tri-) are targeted to the same genomic regions of silent chromatin.

Monomethylated H4 Lys-20 and H3 Lys-9 Are Targeted to the Same Nucleosome in Vivo—The findings above suggested that corresponding methylated states of H4 Lys-20 and H3 Lys-9 would be enriched within the same nucleosomal core particle, especially the mono- and trimethylated forms. To determine this, immunoprecipitations were performed with the mono- or trimethyl-specific H4 Lys-20 antibodies on mononucleosomes prepared from HeLa cells (Fig. 5). Following the immunoprecipitation, Western analysis of the antibody-bound material was performed to verify the enrichment of each modification. Indeed, the monomethyl H4 Lys-20 antibody specifically enriched for nucleosomes containing this modification, whereas di- and trimethylated H4 Lys-20 were not (Fig. 5A). Similarly, the H4 Lys-20 trimethyl-specific antibody enriched for nucleosomes containing this modification but not for the mono- or dimethylated H4 Lys-20 nucleosomes (Fig. 5C). Although similar experiments were attempted with the H4 Lys-20 dimethyl-specific antibodies, we were unsuccessful in obtaining nucleosomes specifically enriched for dimethylated H4 Lys-20. Western analyses were performed on the immunoprecipitated material using the H3 Lys-9

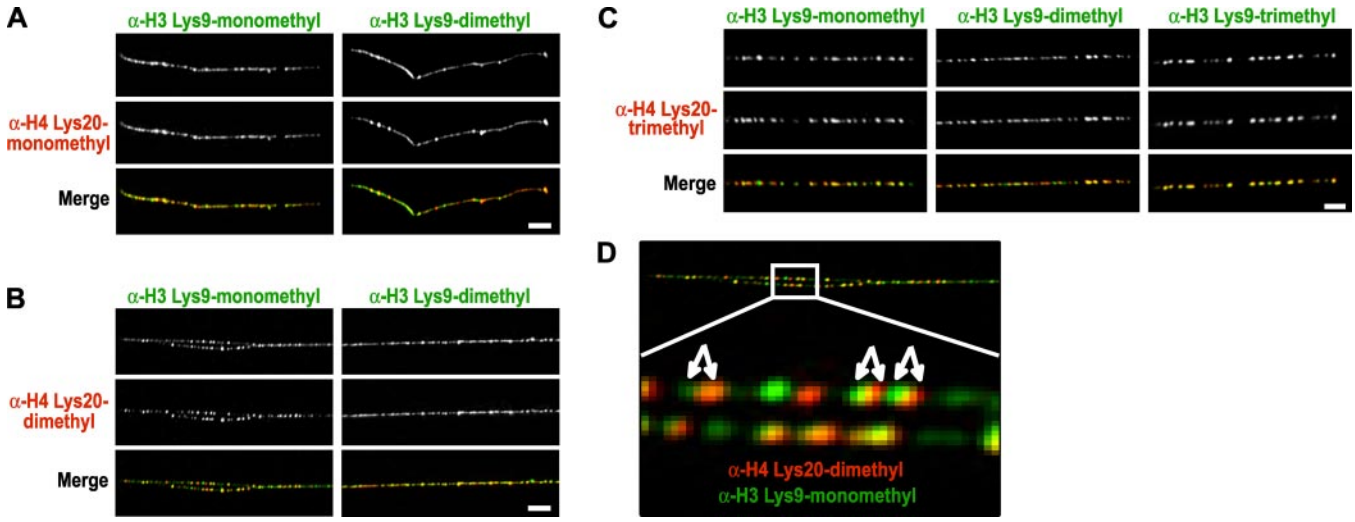

FIGURE 4. **Histone H4 Lys-20 and Histone H3 Lys-9 patterns of methylation are found in similar genomic regions along extended chromatin fibers.** *A*, extended chromatin fibers from HeLa cells were co-stained for monomethylated H4 Lys-20 (Cy3; *red*) and either mono- (left panels) or dimethylated (right panels) H3 Lys-9 (FITC; *green*). Monomethylated H4 Lys-20 preferentially co-localizes to monomethylated H3 Lys-9 regions along chromatin fibers as seen by *yellow* in the merged image. In contrast, monomethylated H4 Lys-20 is largely excluded from regions enriched in dimethylated H3 Lys-9. *B*, chromatin fibers co-stained for dimethylated H4 Lys-20 (Cy3; *red*) and either mono- (left panels) or dimethylated (right panels) H3 Lys-9 (FITC; *green*). Dimethylated H4 Lys-20 preferentially co-localizes to dimethylated H3 Lys-9 regions along the chromatin fibers (*yellow* in the merged image) and is excluded from regions enriched in monomethylated H3 Lys-9 (see *panel D*). *C*, HeLa chromatin fibers co-stained for trimethylated H4 Lys-20 (Cy3; *red*) and the different methylated states of H3 Lys-9 (FITC; *green*). Trimethylated H4 Lys-20 and H3 Lys-9 are enriched within the same regions along the length of the fiber, whereas mono- and dimethylated H3 Lys-9 co-localize less frequently. *D*, enlargement of *panel B* demonstrating that dimethylated H4 Lys-20 and monomethylated H3 Lys-9 flank each other along the chromatin fiber (*arrows*). *Bar* = 2.5 μm.

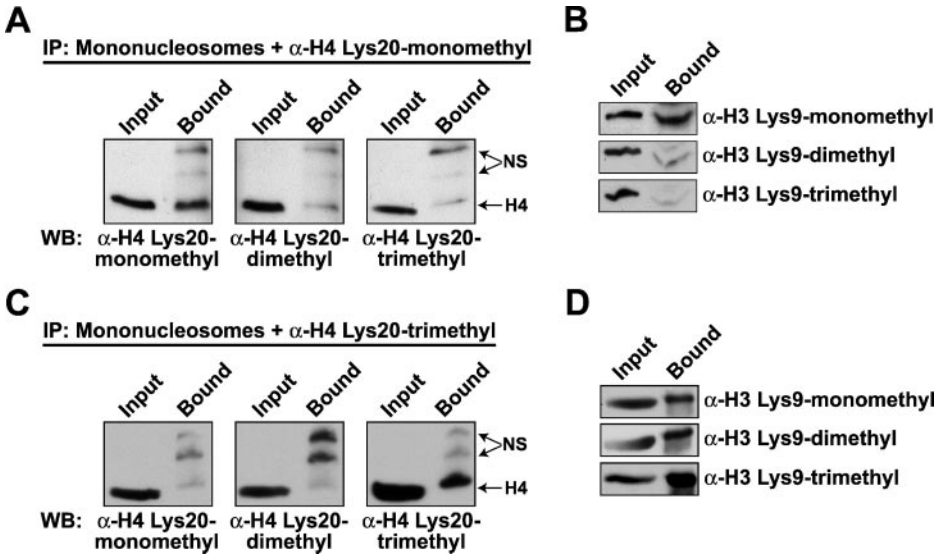

FIGURE 5. **Preferential and selective enrichment of monomethylated H4 Lys-20 and H3 Lys-9 on the same nucleosomal core particle *in vivo*.** *A*, mononucleosomes prepared from HeLa cells were immunoprecipitated (*IP*) with the H4 Lys-20 monomethyl-specific antibody. Western analysis (*WB*) of 2% of the input material and 5% of the eluted bound material indicates that the immunoprecipitated nucleosomes are specifically enriched for the monomethylated form of H4 Lys-20. *NS* represents nonspecific signal most likely generated by performing both the immunoprecipitation and the Western analysis with rabbit polyclonal antibodies. *B*, Western analysis of the H4 Lys-20 monomethyl-enriched nucleosomes indicates that they are also selectively enriched for monomethylated H3 Lys-9. *C*, mononucleosomes were immunoprecipitated with the H4 Lys-20 trimethyl-specific antibody. Western analysis of 2% of the input material and 5% of the eluted bound material indicates that the immunoprecipitated nucleosomes are specifically enriched for the trimethylated form of H4 Lys-20. *D*, Western analysis of the H4 Lys-20 trimethyl-enriched nucleosomes indicates that there is a preferential enrichment for trimethylated H3 Lys-9 *in vivo*, although the mono- and dimethylated forms of H3 Lys-9 are also detected to a lesser extent. Consistent results were obtained in three independent immunoprecipitations for each methyl-specific antibody.

methyl-specific antibodies. Consistent with the immunofluorescence data, monomethylated H3 Lys-9 was exclusively detected in nucleosomes containing monomethylated H4 Lys-20; di- and trimethylated H3 Lys-9 were not detected within these nucleosomes (Fig. 5*B*). Similar to the chromatin fiber findings, trimethylated H3 Lys-9 was preferentially detected in the H4 Lys-20 trimethyl-enriched nucleosomes; however, mono- and dimethylated H3 Lys-9 were also detected, albeit to a far lesser extent (Fig. 5*D*). Although the importance of these results remains unclear, it reinforces our findings that only the monomethylated forms of H4 Lys-20 and H3 Lys-9 were specifically enriched within the same nucleosomal core particle. Therefore, a trans-tail histone code involving these two repressive marks is associated with distinct regions of silent chromatin.

DISCUSSION

Although histones have long been known to be methylated *in vivo*, the exact biological importance of this modification has remained elusive (31). In this study, we sought to further the current understanding

of the biological role(s) of the mono-, di-, and trimethylated forms of H4 Lys-20, the first described methylated histone lysine residue (8). To this end, we successfully created a novel panel of H4 Lys-20 methyl-specific antibodies that, remarkably, do not cross-react with the other methyl modifications on Lys-20, nor are they inhibited by the neighboring acetylation of H4 Lys-16 (Fig. 1). These methyl-specific antibodies were used to determine that each methylated form of H4 Lys-20 partitions to distinct nuclear compartments that appear, at least by indirect immunofluorescence, to be excluded from transcriptionally engaged chromatin (Fig. 2). As we had previously demonstrated, different HMTs are responsible for the specific level of methylation of a specific histone residue *in vivo* (24). Therefore, these findings strongly suggest that the HMTs, themselves, are targeted to distinct genomic regions, by unknown mechanisms, to create these histone marks, which ultimately result in distinct transcriptionally repressive chromatin states.

A recent report described that monomethylated H4 Lys-20 was associated with transcriptionally active chromatin as determined by co-localization with RNA pol II and hyperacetylated H4 using indirect immunofluorescence in mouse erythroleukemia cells (32). Chromatin immunoprecipitation analysis of the β-major region, a gene that is dramatically up-regulated during Me_2SO-induced differentiation of mouse erythroleukemia cells (33), demonstrated a 3–4-fold increase in monomethylated H4 Lys-20 at the β-major promoter and second exon in differentiated mouse erythroleukemia cells when compared with non-differentiated cells. In contrast to these findings, our results are in agreement with several independent reports that monomethylated H4 Lys-20 is associated with transcriptionally silent chromatin in higher eukaryotes (10, 11, 18, 19, 29, 34). Although the reason for this discrepancy is unclear, it does reinforce recent observations that specific histone modifications can also be associated with a juxtaposed DNA-templated process, at least in mouse erythroid cells. For example, it was demonstrated that trimethylated H3 Lys-9, which has become a benchmark of repressed chromatin, was enriched within the actively transcribed regions (but not promoters) of several inducible genes, including β-major, in mouse cells of erythroid lineage (35). Therefore, although we find that the majority of monomethylated H4 Lys-20 is associated with repressed chromatin (Fig. 2), it may also serve an additional role in the active transcription of mouse genes associated with erythroid differentiation. It is unknown whether these observations are valid for other classes of genes and/or in different cell types; further experiments are required to delineate this.

Consistent with previous reports, we found trimethylated H4 Lys-20 enriched within the major and minor satellite repeats of pericentric heterochromatin (19). These findings imply that this modification may specifically mark regions of constitutive heterochromatin, regions that are believed to always be repressed (36). We observed that the bulk of monomethylated H4 Lys-20 was enriched within silent regions of the chromosome arms and was also enriched within the female inactive X chromosome (Figs. 2*A* and 3*B*). These findings imply that this modification may specifically mark regions of facultative heterochromatin, chromatin that is silent but has the faculty to become active. If this is true, where does dimethylated H4 Lys-20 fit into the defined types of heterochromatin? This repressive modification is clearly independent of mono- and trimethylated H4 Lys-20, and therefore, constitutive and facultative heterochromatin (Fig. 2). Based on this, it is conceivable that dimethylated H4 Lys-20 may define an entirely unique type of heterochromatin that has not yet been described. The discovery of the HMT responsible for H4 Lys-20 dimethylation will provide key insights into this theory.

Because we had previously observed similar nuclear compartmentalization of the different methylated states of H3 Lys-9 (24), we hypothesized that both modifications would partition together within these silent regions. Indeed, by employing several techniques, our findings indicate that the corresponding methylated states of H4 Lys-20 and H3 Lys-9 tend to localize to the same silent compartments in the nucleus (Fig. 3) and within the same genomic regions on chromatin fibers (Fig. 4). Analysis at the nucleosomal level revealed that monomethylated H4 Lys-20 and H3 Lys-9 were preferentially and selectively enriched on the same nucleosome core particle *in vivo*. Collectively, these findings indicate that a trans-tail histone code exists in the mammalian nucleus whereby monomethylated H4 Lys-20 and H3 Lys-9 occur on the same nucleosome to mark a distinct repressive chromatin state. To date, there are three other descriptions of trans-tail histone codes involving H2B ubiquitination and H3 Lys-4 methylation (37, 38) or H3 Lys-79 methylation (39, 40) in yeast and another regarding trimethylation of H4 Lys-20 and H3 Lys-9 in mammals (12). We describe a unique trans-tail histone code involving monomethylated H4 Lys-20 and H3 Lys-9 and demonstrate, for the first time, that the modifications occur on the same nucleosome *in vivo*.

A recent study supports our conclusion of a monomethyl H4 Lys-20 and H3 Lys-9 trans-tail histone code (19). Examination of repetitive elements in mouse embryonic stem cells revealed specific patterns of enrichment for specific methyl modifications within different elements. The selective enrichment of both monomethylated H4 Lys-20 and monomethylated H3 Lys-9 was observed in SINE B1 elements, whereas the di- and trimethylated forms of H4 Lys-20 or H3 Lys-9 were not detected. Importantly, both monomethyl modifications were absent at satellite repeats and other retrotransposons, DNA and RNA transposons. Similar to our findings, this type of mutual enrichment and exclusion seemed to be observed only for monomethylation. Although trimethylated H4 Lys-20 and H3 Lys-9 were both strongly enriched within satellite repeats, their degrees of enrichment varied greatly within other repetitive elements. For example, trimethylated H3 Lys-9 was enriched within DNA transposons where trimethylated H4 Lys-20 was lacking, and trimethylated H4 Lys-20 was enriched within retrotransposons and RNA transposons where trimethylated H3 Lys-9 was barely detected. This is consistent with our findings that there was a preferential targeting of trimethylated H4 Lys-20 and H3 Lys-9 on chromatin fibers (Fig. 4*C*) and mononucleosomes (Fig. 5*D*) but that mono- and dimethylated H3 Lys-9 could also be detected, albeit to a far lesser extent.

Despite these findings, recent evidence indicates that there is a trimethyl H4 Lys-20 and H3 Lys-9 trans-tail histone code operating specifically at pericentric heterochromatin (12). In this case, the lack of the Suv39h HMTs resulted in the expected loss of trimethylated H3 Lys-9 but also resulted in the unexpected loss of trimethylated H4 Lys-20 within pericentric regions. These findings indicate that the trimethylation of H4 Lys-20 is dependent upon the prior trimethylation of H3 Lys-9. Similarly, in yeast, the methylation of both H3 Lys-4 and Lys-79 are dependent upon the prior ubiquitination of H2B Lys-123 by Rad6 (37–40). Therefore, in all reported cases regarding trans-tail histone codes, there is a defined unidirectional temporal sequence of modification events. We predict that, based on the model established for trimethylation, the monomethylation of H3 Lys-9 precedes monomethylation of H4 Lys-20, although this has yet to be experimentally determined. Although our findings define a novel trans-tail histone code associated with a distinct type of repressed chromatin, the exact biological function(s) of this phenomenon are currently unknown. The elucidation of the molecular players as well as the genomic targets of this

pathway will be critical to understanding the importance of the monomethylated H4 Lys-20 and H3 Lys-9 trans-tail histone code.

Acknowledgments—We thank Patrick Grant for the purified NuA4 complex and histone acetyl-transferase protocol; Susan Forsburg, Douglas Luche, Angel Tabancay, Jr., and William Dolan for use of the Delta Vision, chromatin fiber protocol, and assistance with fiber imaging; and the USC/Norris Comprehensive Cancer Center Cell and Tissue Imaging Core (2 CA 014089-31) and members of the Rice laboratory for helpful suggestions and comments.

REFERENCES

1. van Holde, K. E. (1988) *Chromatin* (Rich, A., ed.) Springer Series in Molecular Biology, Springer-Verlag New York Inc., New York
2. Wolffe, A. P., and Hayes, J. J. (1999) *Nucleic Acids Res.* **27,** 711–720
3. Peterson, C. L., and Laniel, M. A. (2004) *Curr. Biol.* **14,** R546–551
4. Jenuwein, T., and Allis, C. D. (2001) *Science* **293,** 1074–1080
5. Strahl, B. D., and Allis, C. D. (2000) *Nature* **403,** 41–45
6. Turner, B. M. (2000) *BioEssays* **22,** 836–845
7. Turner, B. M. (2002) *Cell* **111,** 285–291
8. Murray, K. (1964) *Biochemistry* **3,** 10–15
9. Zhang, K., and Tang, H. (2003) *J. Chromatogr. B. Analyt. Technol. Biomed. Life Sci.* **783,** 173–179
10. Fang, J., Feng, Q., Ketel, C. S., Wang, H., Cao, R., Xia, L., Erdjument-Bromage, H., Tempst, P., Simon, J. A., and Zhang, Y. (2002) *Curr. Biol.* **12,** 1086–1099
11. Nishioka, K., Rice, J. C., Sarma, K., Erdjument-Bromage, H., Werner, J., Wang, Y., Chuikov, S., Valenzuela, P., Tempst, P., Steward, R., Lis, J. T., Allis, C. D., and Reinberg, D. (2002) *Mol. Cell* **9,** 1201–1213
12. Schotta, G., Lachner, M., Sarma, K., Ebert, A., Sengupta, R., Reuter, G., Reinberg, D., and Jenuwein, T. (2004) *Genes Dev.* **18,** 1251–1262
13. Couture, J. F., Collazo, E., Brunzelle, J. S., and Trievel, R. C. (2005) *Genes Dev.* **19,** 1455–1465
14. Xiao, B., Jing, C., Kelly, G., Walker, P. A., Muskett, F. W., Frenkiel, T. A., Martin, S. R., Sarma, K., Reinberg, D., Gamblin, S. J., and Wilson, J. R. (2005) *Genes Dev.* **19,** 1444–1454
15. Yin, Y., Liu, C., Tsai, S. N., Zhou, B., Ngai, S. M., and Zhu, G. (2005) *J. Biol. Chem.* **280,** 30025–30031
16. Biron, V. L., McManus, K. J., Hu, N., Hendzel, M. J., and Underhill, D. A. (2004) *Dev. Biol.* **276,** 337–351
17. Julien, E., and Herr, W. (2004) *Mol. Cell* **14,** 713–725
18. Karachentsev, D., Sarma, K., Reinberg, D., and Steward, R. (2005) *Genes Dev.* **19,** 431–435
19. Martens, J. H., O'Sullivan, R. J., Braunschweig, U., Opravil, S., Radolf, M., Steinlein, P., and Jenuwein, T. (2005) *EMBO J.* **24,** 800–812
20. Rice, J. C., Nishioka, K., Sarma, K., Steward, R., Reinberg, D., and Allis, C. D. (2002) *Genes Dev.* **16,** 2225–2230
21. Stadler, F., Kolb, G., Rubusch, L., Baker, S. P., Jones, E. G., and Akbarian, S. (2005) *J. Neurochem.* **94,** 324–336
22. Sanders, S. L., Portoso, M., Mata, J., Bahler, J., Allshire, R. C., and Kouzarides, T. (2004) *Cell* **119,** 603–614
23. Peters, A. H., Kubicek, S., Mechtler, K., O'Sullivan, R. J., Derijck, A. A., Perez-Burgos, L., Kohlmaier, A., Opravil, S., Tachibana, M., Shinkai, Y., Martens, J. H., and Jenuwein, T. (2003) *Mol. Cell* **12,** 1577–1589
24. Rice, J. C., Briggs, S. D., Ueberheide, B., Barber, C. M., Shabanowitz, J., Hunt, D. F., Shinkai, Y., and Allis, C. D. (2003) *Mol. Cell* **12,** 1591–1598
25. Sullivan, B. A., and Karpen, G. H. (2004) *Nat. Struct. Mol. Biol.* **11,** 1076–1083
26. Perez-Burgos, L., Peters, A. H., Opravil, S., Kauer, M., Mechtler, K., and Jenuwein, T. (2004) *Methods Enzymol.* **376,** 234–254
27. Allard, S., Utley, R. T., Savard, J., Clarke, A., Grant, P., Brandl, C. J., Pillus, L., Workman, J. L., and Cote, J. (1999) *EMBO J.* **18,** 5108–5119
28. Grant, P. A., Duggan, L., Cote, J., Roberts, S. M., Brownell, J. E., Candau, R., Ohba, R., Owen-Hughes, T., Allis, C. D., Winston, F., Berger, S. L., and Workman, J. L. (1997) *Genes Dev.* **11,** 1640–1650
29. Kohlmaier, A., Savarese, F., Lachner, M., Martens, J., Jenuwein, T., and Wutz, A. (2004) *PLoS Biol.* **2,** E171
30. Kourmouli, N., Jeppesen, P., Mahadevhaiah, S., Burgoyne, P., Wu, R., Gilbert, D. M., Bongiorni, S., Prantera, G., Fanti, L., Pimpinelli, S., Shi, W., Fundele, R., and Singh, P. B. (2004) *J. Cell Sci.* **117,** 2491–2501
31. Rice, J. C., and Allis, C. D. (2001) *Curr. Opin. Cell Biol.* **13,** 263–273
32. Talasz, H., Lindner, H. H., Sarg, B., and Helliger, W. (2005) *J. Biol. Chem.* **280,** 38814–38822
33. Sawado, T., Igarashi, K., and Groudine, M. (2001) *Proc. Natl. Acad. Sci. U. S. A.* **98,** 10226–10231
34. Vaquero, A., Scher, M., Lee, D., Erdjument-Bromage, H., Tempst, P., and Reinberg, D. (2004) *Mol. Cell* **16,** 93–105
35. Vakoc, C. R., Mandat, S. A., Olenchock, B. A., and Blobel, G. A. (2005) *Mol. Cell* **19,** 381–391
36. Hennig, W. (1999) *Chromosoma* (*Berl.*) **108,** 1–9
37. Dover, J., Schneider, J., Tawiah-Boateng, M. A., Wood, A., Dean, K., Johnston, M., and Shilatifard, A. (2002) *J. Biol. Chem.* **277,** 28368–28371
38. Sun, Z. W., and Allis, C. D. (2002) *Nature* **418,** 104–108
39. Briggs, S. D., Xiao, T., Sun, Z. W., Caldwell, J. A., Shabanowitz, J., Hunt, D. F., Allis, C. D., and Strahl, B. D. (2002) *Nature* **418,** 498
40. Ng, H. H., Xu, R. M., Zhang, Y., and Struhl, K. (2002) *J. Biol. Chem.* **277,** 34655–34657